Turbulence, Heat and Mass Transfer 10

Assessment of Grey-Area Mitigation Techniques and their effects on Jet Aerodynamics and AeroAcoustics

J. Ruano[1], A. Duben[2], A. Gorobets[2] and F.X. Trias[1]
[1]*Heat and Mass Transfer Technological Center (CTTC),*
Universitat Politècnica de Catalunya BarcelonaTech (UPC) ESEIAAT
Colom 11, 08222, Terrassa, Barcelona, Spain
jesus.ruano@upc.edu, francesc.xavier.trias@upc.edu
[2]*Keldysh Insitute of Applied Mathematics (KIAM)*
4A, Miusskaya Sq., Moscow, 125047, Russia
aduben@keldysh.ru gorobets@keldysh.ru

Abstract – This work explores different grey-area mitigation (GAM) methods towards achieving precise aerodynamics and aeroacoustics results of the subsonic turbulent round jet. The GAM technique used is based on a combination of 2D detecting LES models and new adapting subgrid length scales. The numerical simulations are carried out on a set of refining meshes using two different scale-resolving codes: NOISEtte and OpenFOAM. The results indicate that all the evaluated combinations offer appropriate accuracy in predicting noise and show the effect of both the numerical scheme and how subgrid eddy viscosity is modelled.

1. Introduction

The standard method employed by the Computational AeroAcoustics (CAA) community involves splitting hydrodynamics and acoustics using two different solvers. The acoustic solver requires as inputs some hydrodynamic variable values that are obtained from solving the Navier-Stokes equations numerically. Consequently, acoustics will not be computed correctly if turbulence or hydrodynamics are not accurately resolved. In this research, we put focus on two main factors that impact the accuracy of the numerical solution utilized by the acoustic solver. These factors include, among all the ones that compose a numerical simulation, the order of numerical discretization of the convective operator and the turbulence model.

Regarding the first issue, as higher-accuracy numerical solutions are preferred by the acoustic solver, high-order schemes are in great demand. Shur et al. [1, 2] and Bogey [3] have simulated subsonic round jets using high-order schemes on structured meshes. However, using such meshes can be challenging when simulating more complex geometries, which are common in industrial problems. A possible alternative is the use of 2nd order low-dissipative schemes, in exchange for requiring finer meshes. Tyacke et al. [4], Fuchs et al. [5], and more recently, Duben et al. [6] have utilized 2nd order schemes in the simulation of transonic turbulent jets. Finally, another alternative is to use 2nd order schemes with extended stencils, i.e., high-accuracy schemes. Duben and Kozubskaya [7] and Duben et al. [6] have employed such schemes in the simulation of transonic turbulent jets.

The second issue concerns turbulence modelling. Specifically, we will be focusing on the family of hybrid RANS-LES models due to their excellent balance between accuracy and computational cost. And more precisely, we restrict this study only to non-zonal DES models. One of the current lines of investigation within non-zonal DES is mitigating the grey-area problem in shear-layer flows, which causes non-physical oscillations that render the results invalid.

The main goal of the Grey-Area Mitigation (GAM) techniques, i.e. avoiding the unphysical delay from the RANS to the LES zone, is achieve a faster transition from steady RANS to the time-dependent part of the mesh working on the LES regime. This transition can be accelerated by decreasing the amount of turbulent viscosity added. Following the usual definition of ν_t:

$$\nu_t = (C_{\mathrm{LES}}\Delta_{\mathrm{SGS}})^2 \cdot \mathscr{D}_{\mathrm{LES}}(\overline{u}), \tag{1}$$

where Δ_{SGS} is the subgrid length scale, $\mathscr{D}_{\mathrm{LES}}$ is the LES model differential operator, $\overline{u}$ is the filtered velocity, and C_{LES} is the LES constant. This relation means that decreasing Δ_{SGS} or $\mathscr{D}_{\mathrm{LES}}$ or even both, will imply also a decrease in the numerical turbulent viscosity. Special subgrid length scale sensitive to the local parameters of the flow, such as Δ_{SLA} [8], $\tilde{\Delta}_{\omega}$ [9], or Δ_{lsq} [10], in conjunction with an LES model sensitive to two-dimensional flow patterns, such as σ, WALE [11], or S3QR [12] are good candidates as a GAM technique as they are able to reduce ν_t thus triggering the RANS-to-LES transition.

This work investigates the effect that different GAM techniques have on the aerodynamics and acoustics of an immersed jet at Reynolds number based on the diameter of $Re_D = 1.1 \cdot 10^6$ and Mach number of $M = 0.9$. As noise at the far-field is very sensitive to the accuracy of the numerical solution of the aerodynamic fields, ν_t must add enough diffusion to avoid spurious noise generation and, at the same time, avoid the delay from RANS to LES regime.

2. Case formulation and computational meshes

As previously said, the herepresented study investigates an immersed jet emerging from a conical nozzle with a Mach number of $M = 0.9$ and a Reynolds number based on the diameter of $Re_D = 1.1 \cdot 10^6$. A set of three refining hexahedral meshes [13, 2, 7, 14] is used to check the convergence of the obtained results. Their main characteristics are summarized in Table 1. Additionally, in order to compute noise, a set of surface meshes where velocity and pressure will be stored are required. Once the hydrodynamic simulation is finished, the values previously stored will be used in the acoustic post-processor to compute noise at given locations. Regarding boundary conditions at the exit of the nozzle, a RANS profile obtained previously is imposed by simulating a pipe flow. This follows a two-stage approach methodology where first the internal part of the nozzle is simulated via RANS, and then the jet plume is simulated in a second simulation.

Table 1: Meshes parameters

Parameter	G1	G2	G3
N_n	1.52M	4.13M	8.87M
N_φ	64	80	160
Δ_x/D at the nozzle exit	0.011	0.008	0.008
$\min(\Delta_r/D)$ in the shear layer	0.003	0.0025	0.0025
$r\Delta_\varphi/D$ in the shear layer	0.05	0.04	0.02

3. Numerical setup

As has been commented on in the introduction, one of the key aspects within CAA is which discrete schemes are used. They can introduce numerical diffusion or not be accurate enough to propagate waves through long distances. For this reason, to assess the impact of numerical scheme accuracy, two different codes were utilized in this work.

The first one is the NOISEtte in-hose code [15]. NOISEtte is based on quasi-1D vertex-centred Edge-Based Reconstruction (EBR) [16]. A blending between central and upwind stencils [7] is used to discretise the convective term [17]. Finally, the acoustic post-processor used is based on FWH method [18] using Farassat formulation [19].

The second code is the open-source software OpenFOAM, based on a collocated unstructured finite-volume approach. As the NOISEtte, OpenFOAM uses a blending of upwind and central schemes in the discretization of the convective term. However, OpenFOAM uses a different blending [20] and second-order schemes instead of high-accuracy ones [7]. Noise is computed using also FWH method but avoiding retarded time formulation by transforming temporal signals into spectral ones. The main differences between codes are summarized in Table 2

Table 2: Details on the numerical parameters used

Characteristic	NOISEtte	OpenFOAM
FVM approach	Vertex-centered	Cell-centered
Hybrid scheme	Guseva et. al., 2017	Travin et. al., 2000
Central scheme	4th order*	2nd order
Upwind scheme	5th order*	2nd order
Time integration	Implicit 2nd order	Implicit 2nd order
FWH equation	Retarded time	Phase shift

*On translationally symmetric meshes

As previously commented, hydrodynamic variables are stored on a set of non-overlapping surface meshes; in the top figure of Figure 1, their location can be seen. In order to improve the convergence of acoustic results and reduce the apparition of spurious noise, the total contribution of each surface is averaged, following Spalart [21] and Shur [1] recommendations.

Regarding turbulence modelling, three different Grey-Area Mitigation techniques were used to study the effect of the RANS-to-LES transition. These GAM strategies involved using combinations of Δ_{SLA} with the Smagorinsky model, $\tilde{\Delta}_{\omega}$ with the σ model and Δ_{lsq} with the S3QR model.

4. Results

In this section, we present and discuss the obtained numerical results. The time-averaged streamwise velocity and its fluctuations, i.e. its root mean square, are compared with Lau et. al. [22, 23], Simonich et. al. [24], Bridges and Wernet [25] and Arakeri et. al. [26]. On the other hand, noise results are compared with Viswanathan [27].

4.1 Aerodynamics

We have included in Figure 1 an instantaneous flow field of both codes in order to see vorticity profiles in the jet plume. However, as *Color Fluid Dynamics* is not enough to fully establish the validity of our results, in Figures 2 and 3 we have included the time-averaged results of the streamwise velocity in the jet centerline as well as its time-averaged fluctuations. The first thing that can be noticed, is that both codes exhibit a clear improvement as meshes become finer as the numerical results trend to the experimental values. NOISEtte produces slightly better results due to using higher-accuracy schemes. However, OpenFOAM results, even using low-order schemes, are also very close to the experimental values, exhibiting a potential zone in Figure 2 a little bit smaller than the one obtained by NOISEtte.

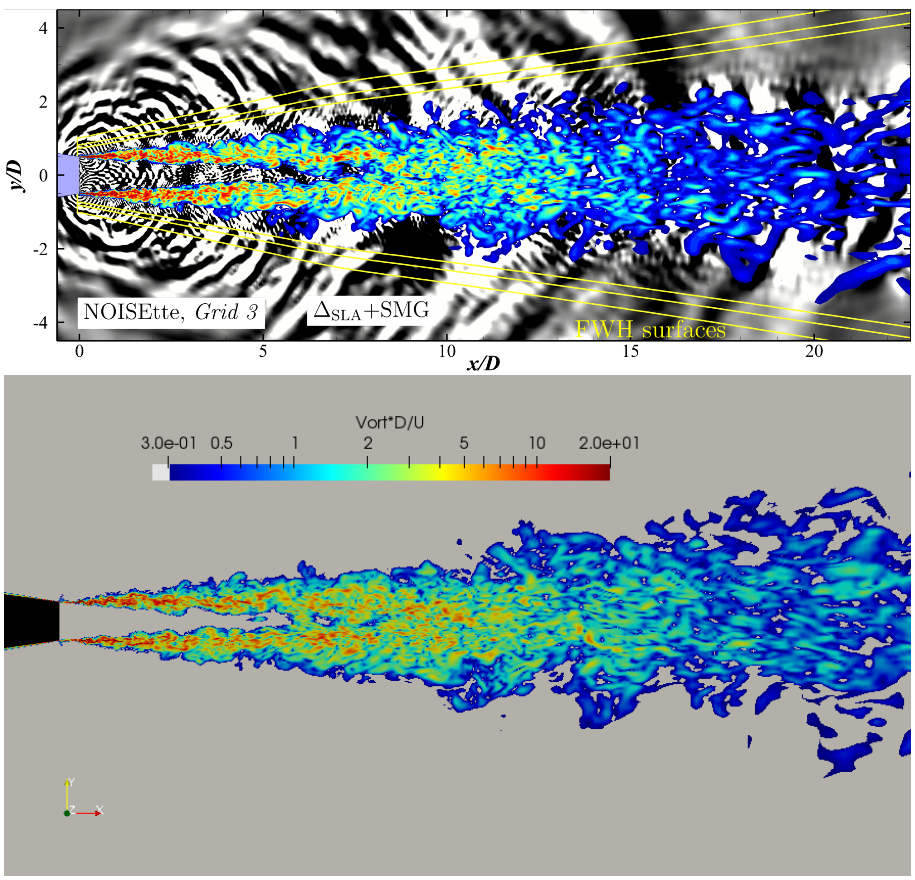

Figure 1: Instantaneous flow field in the jet-plume region, with the yellow lines marking the location of the FWH control surfaces. NOISEtte results at the top and OpenFOAM results at the bottom.

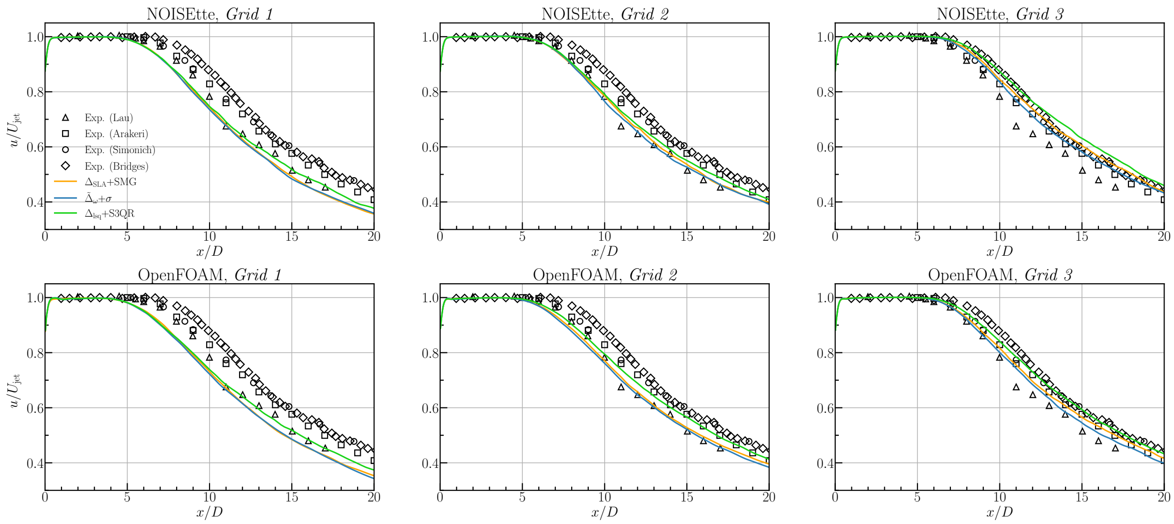

Figure 2: Centerline distributions of the streamwise velocity on a set of refining meshes. NOISEtte results at the top and OpenFOAM results at the bottom.

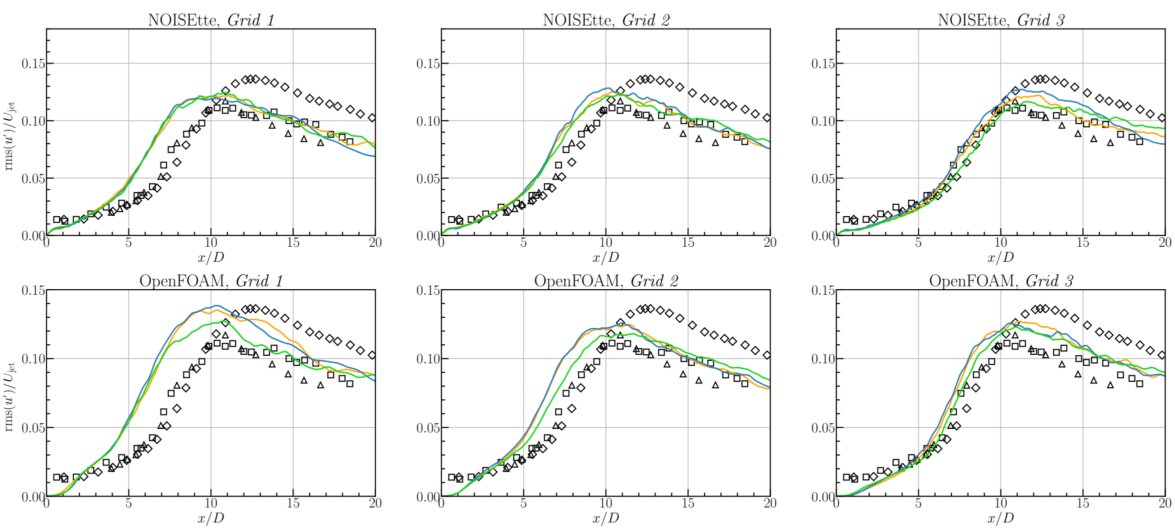

Figure 3: Centerline distributions of the streamwise velocity pulsations on a set of refining meshes. NOISEtte results at the top and OpenFOAM results at the bottom.

The streamwise velocity fluctuations, plot in Figure 3, also show the expected mesh convergence as the numerical results become closer to the experimental reference data. Concerning these reference data, for values of $x/D >$10 two different trends appear; numerical results seem to be always in the region between the region that is formed by those two trends. It should be also noted that, while NOISEtte results in Figure 3 are very similar for all the considered GAM techniques, OpenFOAM results seem to have differences, being more noticeable in Grid 1 and Grid 2. As can be seen, $\Delta_{lsq}+S3QR$ results are slightly different than the ones obtained with the other approaches. This could be explained by the fact that Δ_{lsq} in the fully developed turbulence region, i.e. $x/D >$5-7, trends to Δ_{Vol} while the other two trend to Δ_{Max}, adding more turbulent viscosity to the simulation.

4.2 Acoustics

As has been commented along this work, obtaining accurate noise results is a more challenging task. In Figure 4 the Overall Sound Pressure Level (OASPL) at different observer angles, i.e. noise directivity, is shown. Similarly to aerodynamic results, the expected mesh convergence is achieved as mesh refinement leads to better agreement between numerical and experimental results.

Both codes seem to suffer from an overprediction of the generated noise at low angles, while slightly underpredicting noise at higher angles. The overprediction is related to spurious noise generated by the non-physical RANS-to-LES transition of the early part of the shear layer. Therefore, as mesh is refined and this transition is better captured, the overprediction is attenuated.

NOISEtte results are more different among them than the ones obtained by OpenFOAM. This is explained by the fact OpenFOAM uses low-order schemes with higher numerical dissipation errors introduced by the upwind part of the convective schemes. In constrast NOISEtte introduces a lesser amount of numerical diffusion via the convective scheme and, consequently, the differences between the selected GAM approaches can be spotted more easily.

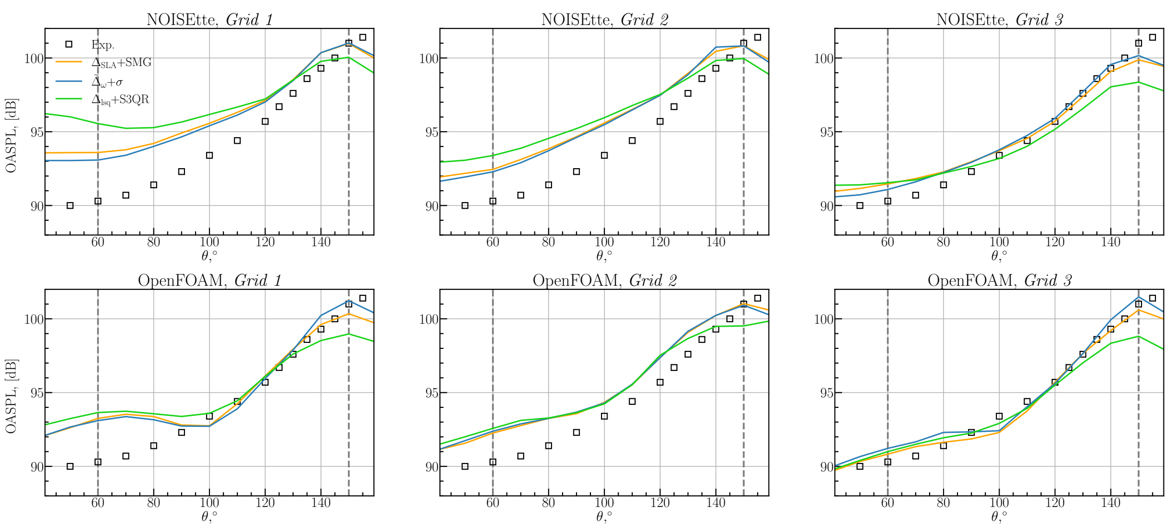

Figure 4: Noise directivity obtained using different approaches. NOISEtte results at top and OpenFOAM results at bottom.

In Figures 5 and 6 the 1/3rd octave spectrums are included. Results at a low observer angle, i.e. Figure 5, using NOISEtte reveal an excellent correlation between numerical and empirical results for Strouhal numbers below 1. Nonetheless, for higher Strouhal, the coarsest mesh presents an purely numerical energy peak. In other words, a numerical noise is generated and contaminates the acoustic directivity obtained in Figure 4. As can be seen, mesh refinement leads to a finer transition between the RANS and LES zones and, consequently, the numerical results are closer to the experimental ones.

On the other hand, the usage of low-order schemes in OpenFOAM help to attenuate the energy peak. This is still present in the results, a little more deviated to Strouhal numbers around 1 instead higher than 1, but the energy contained is reduced. As previously commented, the usage of more dissipative schemes makes the results of the different GAM techniques more similar than when high-accuracy and low-dissipation ones are employed. It should be noticed also that spectrums in OpenFOAM start to decay earlier than in the plots from NOISEtte, making the effective resolution of OpenFOAM a little bit smaller than NOISEtte.

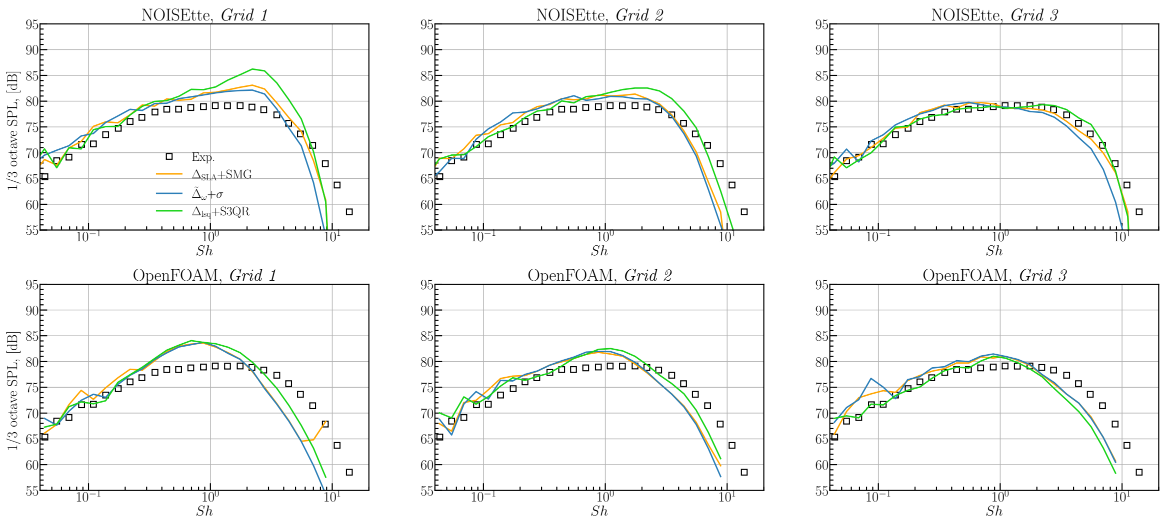

Figure 5: 1/3rd-octave integrated spectrums at the observer angle $\theta = 60°$.

To analyse the shared noise underprediction for all the selected approaches, the results at higher observer angles are presented in Figure 6.

NOISEtte results in Figure 4 for higher observer angles show an almost exact match between numerical and empirical results. Ironically, the finer mesh is the one with a higher mismatch between numerical and empirical data. In the Strouhal range between 0.2-0.9, there is a small underprediction for all the selected GAM approaches, being more noticeable when Δ_{lsq}+S3QR approach is used. This is exactly what can be observed in Figure 4, which is an integrated version of the 1/3rd spectrums of the different observer angles, where for higher observer angles the Δ_{lsq}+S3QR approach has the worst correlation between empirical and numerical results. Nonetheless, such high observer angles, almost in the jet zone, are not crucial in determining the validity or not of a GAM technique.

On the other hand, OpenFOAM results in all the considered approaches, are underpredicted in the whole Strouhal range. Noise at higher observer angles is produced mainly by the big vortices travelling downstream of the domain. As the numerical diffusion introduced by the convective scheme used by OpenFOAM is higher than the one introduced by high-accuracy schemes, the vortices responsible for noise generation are attenuated. Therefore, as they are not so energetic, they cannot produce the expected noise levels.

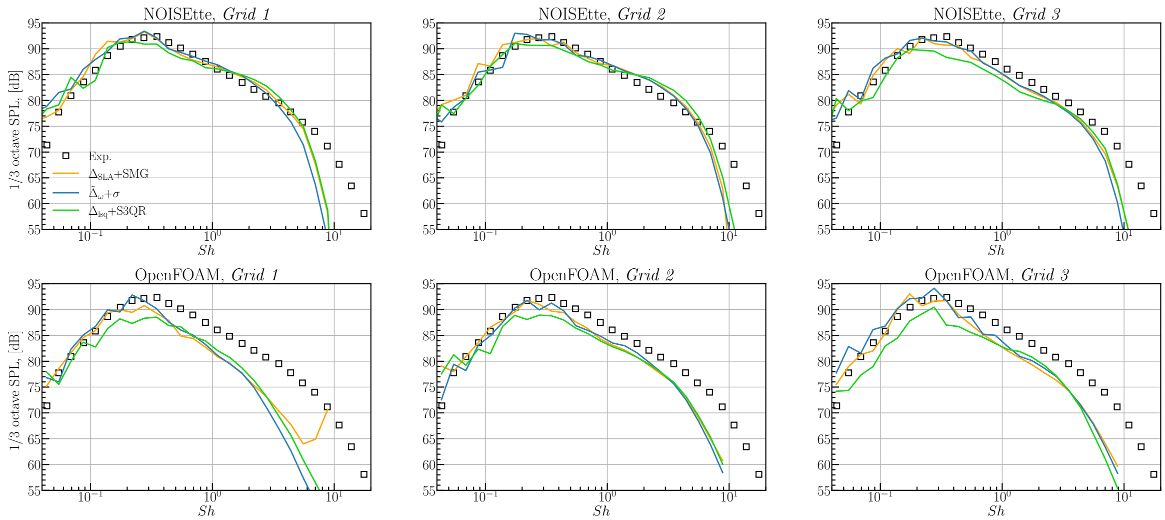

Figure 6: 1/3rd-octave integrated spectrums at the observer angle $\theta = 150°$.

5. Concluding remarks

The numerical results of an immersed subsonic round jet using two different codes have been presented. The main conclusion which can be extracted from the presented results is that GAM techniques are of extreme importance in order to achieve good hydrodynamic and, specifically, acoustic results.

Regarding hydrodynamic results, high-accuracy schemes have demonstrated a better correlation with empirical data than if the 2nd order schemes used by OpenFOAM are selected. However, results obtained by OpenFOAM cannot be considered inaccurate at all as they present minor differences with the ones obtained by NOISEtte.

The differences in the hydrodynamic results obtained by the selected GAM techniques have been explained by the behaviour of the subgrid length scale in the fully developed turbulent region. Δ_{lsq} trends to Δ_{Vol} whereas the other two selected length scales trend to Δ_{Max}. These differences become more noticeable when high-accuracy schemes are used, as the amount of numerical diffusion they introduce is minimal.

Acoustic results using both codes have shown the expected mesh convergence. Differently from hydrodynamic results, acoustics have shown to be more dependent on the selected GAM approach. Low observer angles have been found to be overestimated due to spurious noise generation in the initial part of the shear layer. Mesh refining has been found to strongly attenuate the overestimation of these angles obtaining numerical results very close to reference data. On the other hand, high-observer angles have been found to be slightly underpredicted. Nonetheless, very high-observer angles almost located in the jet region should not be used as a decisive factor to assess the validity of the different GAM techniques.

References

1. M. L. Shur, P. R. Spalart, and M. K. Strelets, “Noise prediction for increasingly complex jets. Part I: Methods and tests,” *International Journal of Aeroacoustics*, vol. 4, pp. 213–245, jul 2005.
2. M. L. Shur, P. R. Spalart, and M. K. Strelets, “Jet noise computation based on enhanced DES formulations accelerating the RANS-to-LES transition in free shear layers,” *International Journal of Aeroacoustics*, vol. 15, pp. 595–613, jul 2016.
3. C. Bogey, “Grid sensitivity of flow field and noise of high-reynolds-number jets computed by large-eddy simulation,” *International Journal of Aeroacoustics*, vol. 17, pp. 399–424, may 2018.
4. J. Tyacke, I. Naqavi, Z.-N. Wang, P. Tucker, and P. Boehning, “Predictive large eddy simulation for jet aeroacoustics–current approach and industrial application,” *Journal of Turbomachinery*, vol. 139, mar 2017.
5. M. Fuchs, C. Mockett, M. Shur, M. Strelets, and J. C. Kok, “Single-stream round jet at m = 0.9,” in *Notes on Numerical Fluid Mechanics and Multidisciplinary Design*, pp. 125–137, Springer International Publishing, jul 2017.
6. A. P. Duben, J. Ruano, A. V. Gorobets, J. Rigola, and F. Xavier Trias, “Evaluation of enhanced gray area mitigation approaches based on jet aeroacoustics,” *AIAA Journal*, vol. 61, no. 2, pp. 612–625, 2023.
7. A. P. Duben and T. K. Kozubskaya, “Evaluation of quasi-one-dimensional unstructured method for jet noise prediction,” *AIAA Journal*, vol. 57, pp. 5142–5155, dec 2019.
8. M. L. Shur, P. R. Spalart, M. K. Strelets, and A. K. Travin, “An enhanced version of DES with rapid transition from RANS to LES in separated flows,” *Flow, Turbulence and Combustion volume*, vol. 95, pp. 709–737, jun 2015.
9. C. Mockett, M. Fuchs, A. Garbaruk, M. Shur, P. Spalart, M. Strelets, F. Thiele, and A. Travin, “Two non-zonal approaches to accelerate RANS to LES transition of free shear layers in DES,” in *Progress in Hybrid RANS-LES Modelling*, pp. 187–201, Springer International Publishing, 2015.
10. F. X. Trias, A. Gorobets, M. H. Silvis, R. W. C. P. Verstappen, and A. Oliva, “A new subgrid characteristic length for turbulence simulations on anisotropic grids,” *Physics of Fluids*, vol. 29, p. 115109, nov 2017.
11. F. Nicoud, H. B. Toda, O. Cabrit, S. Bose, and J. Lee, “Using singular values to build a subgrid-scale model for large eddy simulations,” *Physics of Fluids*, vol. 23, p. 085106, aug 2011.
12. F. X. Trias, D. Folch, A. Gorobets, and A. Oliva, “Building proper invariants for eddy-viscosity subgrid-scale models,” *Physics of Fluids*, vol. 27, p. 065103, jun 2015.
13. M. Shur, P. Spalart, and M. Strelets, “LES-based evaluation of a microjet noise reduction concept in static and flight conditions,” *Procedia Engineering*, vol. 6, pp. 44–53, 2010.
14. A. Pont-Vílchez, A. Duben, A. Gorobets, A. Revell, A. Oliva, and F. X. Trias, “New strategies for mitigating the gray area in delayed-detached eddy simulation models,” *AIAA Journal*, vol. 59, pp. 3331–3345, sep 2021.
15. A. Gorobets, “Parallel algorithm of the NOISEtte code for CFD and CAA simulations,” *Lobachevskii Journal of Mathematics*, vol. 39, pp. 524–532, may 2018.
16. I. Abalakin, P. Bakhvalov, and T. Kozubskaya, “Edge-based reconstruction schemes for unstructured tetrahedral meshes,” *International Journal for Numerical Methods in Fluids*,

vol. 81, pp. 331–356, dec 2015.

17. E. K. Guseva, A. V. Garbaruk, and M. K. Strelets, "An automatic hybrid numerical scheme for global RANS-LES approaches," *Journal of Physics: Conference Series*, vol. 929, p. 012099, nov 2017.
18. "Sound generation by turbulence and surfaces in arbitrary motion," *Philosophical Transactions of the Royal Society of London. Series A, Mathematical and Physical Sciences*, vol. 264, pp. 321–342, may 1969.
19. F. Farassat, "Linear acoustic formulas for calculation of rotating blade noise," *AIAA Journal*, vol. 19, pp. 1122–1130, sep 1981.
20. A. Travin, M. Shur, M. Strelets, and P. R. Spalart, "Physical and numerical upgrades in the detached-eddy simulation of complex turbulent flows," in *Fluid Mechanics and Its Applications*, pp. 239–254, Springer Netherlands, 2002.
21. P. R. Spalart and M. L. Shur, "Variants of the ffowcs williams - hawkings equation and their coupling with simulations of hot jets," *International Journal of Aeroacoustics*, vol. 8, pp. 477–491, jul 2009.
22. J. C. Lau, P. J. Morris, and M. J. Fisher, "Measurements in subsonic and supersonic free jets using a laser velocimeter," *Journal of Fluid Mechanics*, vol. 93, pp. 1–27, jul 1979.
23. J. C. Lau, "Effects of exit mach number and temperature on mean-flow and turbulence characteristics in round jets," *Journal of Fluid Mechanics*, vol. 105, p. 193, apr 1981.
24. J. Simonich, S. Narayanan, T. Barber, and M. Nishimura, "High subsonic jet experiments. i - aeroacoustic characterization, noise reduction and dimensional scaling effects," in *6th Aeroacoustics Conference and Exhibit*, American Institute of Aeronautics and Astronautics, jun 2000.
25. J. Bridges and M. Wernet, "Establishing consensus turbulence statistics for hot subsonic jets," in *16th AIAA/CEAS Aeroacoustics Conference*, American Institute of Aeronautics and Astronautics, jun 2010.
26. V. H. Arakeri, A. Krothapalli, V. Siddavaram, M. B. Alkislar, and L. M. Lourenco, "On the use of microjets to suppress turbulence in a mach 0.9 axisymmetric jet," *Journal of Fluid Mechanics*, vol. 490, pp. 75–98, sep 2003.
27. K. Viswanathan, "Aeroacoustics of hot jets," *Journal of Fluid Mechanics*, vol. 516, pp. 39–82, oct 2004.